Oceanologia, 68 (4)/2026, 68407
Polish Academy of Sciences
Institute of Oceanology
Open access article under the CC BY license
https://doi.org/10.5697/RMQJ1494

Nutrient dynamics and biogeochemical fluxes in a pristine tropical hypertidal estuary: the Turiaçu River, Brazil

Carlos Noriega[1,*], Mauricio Costa[2], Rafael Aquino[2], Sury Monteiro[2], Iranilson Silva[2], Leandro Santana[2], Rayane Menezes[2], Carmen Medeiros[1], Moacyr Araujo[1, 3], Marcelo Rollnic[2]

Abstract

The Turiaçu River estuary (Brazil) is a tropical "false ria" with a hypertidal regime and low anthropogenic pressure. Observations revealed pronounced salinity variability (2–30 psu) driven by tidal forcing and high freshwater discharge, with pH ranging from slightly acidic to alkaline (5.0–9.0) and dissolved oxygen levels often below regulatory thresholds (mean <5.0 mg L^{-1}). Persistent high turbidity (>100 NTU) regulated oxygen and nutrient dynamics, while chlorophyll *a* concentrations remained low (mean 7.8 mg m^{-3}), indicating light limitation of primary production. Nutrient distributions exhibited non-conservative behaviour along the salinity gradient, with N:P ratios consistently below Redfield proportions (mean $DIN : SiO_2 : {PO_4}^{3-} = 13 : 178 : 1$), indicating nitrogen limitation. Biogeochemical modelling revealed that the system generally exports dissolved inorganic phosphorus and nitrogen to coastal waters, with net ecosystem metabolism alternating seasonally between heterotrophy (during high river discharge) and autotrophy (during low discharge). Denitrification dominated nitrogen removal during the wet season, while nitrogen fixation prevailed in the dry season. Overall, hydrodynamics – driven by tidal energy and seasonal freshwater input – remain the primary biogeochemical control in this pristine hypertidal system.

Keywords
False ria; Amazonian coast; Turbidity; Water quality; Nutrient export; Seasonal variability

[1] *Department of Oceanography, Federal University of Pernambuco – UFPE, Av. Arquitetura s/n, 50740–550, Recife, Brazil*
[2] *Laboratório de Pesquisa e Monitoramento Ambiental Marinho (LAPMAR), Federal University of Pará, Belém, Brazil*
[3] *Brazilian Research Network on Global Climate Changes – Rede CLIMA, São José dos Campos, Brazil*
***Correspondence**: cnoriega.ufpe@gmail.com (C. Noriega)

Received: 11 January 2026; **revised:** 29 July 2026; **accepted**: 3 November 2026

List of abbreviations, symbols, and acronyms

- ANA – Agência Nacional das Águas (Brazilian National Water Agency)
- CONAMA – Conselho Nacional do Meio Ambiente (Brazilian National Council on the Environment)
- DIN – Dissolved Inorganic Nitrogen
- DINX – Dissolved Inorganic Nitrogen eXcess index
- DIP – Dissolved Inorganic Phosphorus
- DIY – Dissolved Inorganic Y (where Y represents Nitrogen or Phosphorus in model budgets)
- DO – Dissolved Oxygen
- IBGE – Instituto Brasileiro de Geografia e Estatística
- INMET – Instituto Nacional de Meteorologia
- ITCZ – Intertropical Convergence Zone
- LAPMAR – Laboratório de Análises de Parâmetros Marinhos (Unit of Laboratory Analysis)
- LOICZ – Land-Ocean Interactions in the Coastal Zone
- NEM – Net Ecosystem Metabolism
- NH_4^+ – Ammonium
- NO_2^- – Nitrite
- NO_3^- – Nitrate

© 2026 The Author(s). This is the Open Access article distributed under the terms of the Creative Commons Attribution Licence.

- NTU – Nephelometric Turbidity Units
- ORP – Oxidation-Reduction Potential
- P – Gross Primary Production
- PO_4^{3-} – Phosphate
- psu – Practical Salinity Units
- R – Ecosystem Respiration
- SiO_2 – Silicate
- VQ – Fluvial discharge in mass balance
- VR – Residual water flow
- Vsys – System volume
- VX – Mixing water flow
- ΔDIN – Non-conservative flux of dissolved inorganic nitrogen
- ΔDIP – Non-conservative flux of dissolved inorganic phosphorus

1. Introduction

Estuaries are key transitional environments that regulate the transfer of water, sediments, nutrients, and organic matter from land to the ocean (Thrush et al., 2013; Araujo et al., 2014; Han et al., 2026). They receive substantial inputs of freshwater, dissolved and particulate organic matter, suspended solids, nutrients, and land-derived contaminants. At the same time, they facilitate the exchange of materials and energy with adjacent coastal waters, thereby playing a central role in coastal biogeochemical cycles (Araujo et al., 2014; Li and Bush, 2015).

Globally, most coastal regions are dominated by microtidal and mesotidal regimes (Costa, 2020). However, a limited number of estuarine systems experience extreme tidal amplitudes, known as hypertides (Figure S1; supplementary material). Archer (2013) classified hypertidal ranges into five subclasses, from 6 to 16 m, reflecting progressively higher tidal energy. These systems are characterized by intense hydrodynamic and sedimentary processes, including erosion, transport, and deposition, which can generate pronounced short-term variability. Hypertidal estuaries are predominantly concentrated in the Northern Hemisphere, particularly in western Europe, while in the Southern Hemisphere they occur mainly in northwest Australia and in Patagonia (Archer, 2013).

The magnitude and temporal variability of these physical processes are largely controlled by freshwater discharge, estuarine morphology, topography, and the fluxes of chemical elements and suspended material (Costa, 2020). In Brazil, several hypertidal systems have been identified, including estuaries in the states of Amapá and Maranhão, such as Igarapé do Inferno, Ilha de Maracá, Mutuoca Bay, the Turiaçu River, and the Golfão Maranhense (El-Robrini et al., 2006; Torres and El-Robrini, 2006).

Understanding hypertidal estuaries is important for both scientific and applied reasons. From a geological perspective, these systems serve as modern analogues for ancient estuaries formed under extreme hydrodynamic conditions. They also represent potential sources of renewable tidal energy and play a critical role in mitigating socio-environmental impacts in coastal zones, particularly with respect to shoreline erosion, saline intrusion, and water quality regulation. Owing to their high-energy regime, hypertidal estuaries typically exhibit elevated concentrations of suspended particulate matter and turbidity, as documented in systems such as the Severn and Isle of Man estuaries (Uncles et al., 2002; Kirby, 2010; Uncles et al., 2013). These conditions strongly influence the transport, transformation, and availability of nutrients, especially nitrogen (N) and phosphorus (P), which may act as important sources of fertilization for adjacent coastal waters.

Unlike mesotidal estuaries, where nutrient dynamics are often controlled by a balance between river discharge and biological uptake within longer residence times, hypertidal systems are expected to exhibit distinct biogeochemical behaviour. The combination of strong tidal currents (~ 1–3 m s^{-1}), elevated suspended particulate matter, and short water residence times should promote: (i) non-conservative additions of dissolved inorganic phosphorus (DIP) and nitrogen (DIN) in the middle and lower estuary due to sediment resuspension and desorption; (ii) net export of most nutrients to the coastal ocean, even during periods of high river discharge; and (iii) light limitation of primary production by persistent turbidity, decoupling nutrient availability from phytoplankton biomass.

Based on these physical controls, we anticipate that the biogeochemical functioning of the Turiaçu estuary will exhibit three distinctive patterns: (i) persistent nitrogen limitation ($N : P < 16 : 1$), as denitrification in the highly turbid mixing zone should remove excess nitrogen relative to phosphorus; (ii) seasonal alternation between net heterotrophy (during high river discharge, when respiration exceeds production) and net autotrophy (during low discharge, when light penetration increases); and (iii) turbidity, rather than nutrient concentration, will emerge as the primary factor controlling phytoplankton biomass, given that light limitation should override nutrient availability in the hypertidal mixing zone.

Despite their relevance, the hydrochemical functioning and nutrient dynamics of tropical hypertidal estuaries remain poorly constrained, particularly in systems subject to low anthropogenic pressure. Most existing studies focus on temperate hypertidal environments or on estuaries strongly affected by human activities, limiting our understanding of baseline biogeochemical conditions in relatively pristine tropical settings.

Unlike the well-documented temperate hypertidal systems or anthropo-genically impacted tropical estuaries (e.g., Guanabara Bay, where dissolved inorganic nitrogen can exceed 50 μmol L^{-1}; Aguiar et al., 2011), the Turiaçu River estuary lacks any historical hydrochemical baseline. This absence of prior data, combined with the system's low population density and extensive mangrove cover, makes it a unique opportunity to characterize the natural biogeochemical functioning of a tropical hypertidal system. Furthermore, the ongoing expansion of agricultural frontiers in the Maranhão region and the projected intensification of the hydrological cycle under climate change underscore the urgency of establishing this pre-impact baseline. Documenting the present-day nutrient dynamics and biogeochemical fluxes will not only fill a critical data gap for hypertidal tropical systems but also provide a reference for future environmental assessments and for validating global nutrient export models (e.g., Global NEWS) that currently rely heavily on temperate datasets.

The Turiaçu River estuary represents a suitable system to address this gap. Its watershed high freshwater discharge (> 200 m^3 s^{-1}), intense rainfall (~ 2000 mm yr^{-1}), and low population density (< 20 inhabitants km^{-2}). Previous studies in the region have focused mainly on water quality in lacustrine environments and the river's fluvial reach (Nogueira, 2003; Santos et al., 2019) or on land-use patterns (Almeida et al., 2022). However, comprehensive investigations addressing seasonal hydrochemical variability, nutrient stoichiometry, and biogeochemical fluxes in the estuarine domain are still lacking. In this context, the quantification of dissolved nutrients (N, P, and silicate) and N : P ratios in a minimally impacted tropical hypertidal estuary provides a valuable reference for comparison with mesotidal and more anthropogenically influenced systems.

The main objective of this study was to evaluate the estuarine dynamics of the Turiaçu River through the seasonal variability of key chemical elements (N, P, and Si) over an annual cycle. In addition, biogeochemical modelling was applied to estimate nutrient fluxes and dominant metabolic processes at the land–ocean interface. By integrating hydrochemical observations with modelling approaches, this study provides a comprehensive characterization of a tropical hypertidal estuary and contributes to a broader understanding of biogeochemical controls in high-energy coastal systems.

2. Material and methods

2.1 Study area

The Turiaçu River estuary is a tropical "false ria" (i.e., a coastal plain estuary formed by partial submergence of a river valley, with a wide mouth but lacking the typical branching morphology of a ria) system (El-Robrini et al., 2006) characterized by numerous abandoned meanders and connectivity with several upstream lagoon bodies (Figure 1). The watershed covers approximately 14,132 km^2 (Bandeira, 2013) and includes extensive mangrove-dominated areas, with the Paruá River and Alto Turi River as its main tributaries. The basin exhibits a marked seasonal climate, with a rainy period from January to July and a dry period from August to December, including transitional phases. Mean annual rainfall is approximately 2140 mm, with most precipitation ($\sim 80\%$) occurring during the first half of the year and a pronounced maximum in April (INMET, 2018).

During the dry season, the estuary is predominantly influenced by southeast trade winds, whereas northeast trade winds prevail during the rainy season, with seasonal differences in wind intensity (INMET, 2018). These variations are primarily associated with the latitudinal migration of the Intertropical Convergence Zone (ITCZ), which governs regional wind patterns. Wind forcing interacts with tidal and riverine processes, modulating circulation, mixing, and material transport within the estuarine system. Turiaçu Bay is subject to a semidiurnal hypertidal regime, representing one of the largest tidal amplitudes in Brazil, with mean spring and neap tidal ranges of 6.65 m and 5.24 m, respectively (FEMAR, 2017). Freshwater input to the estuary is mainly supplied by the Paruá and Alto Turi rivers, with average annual discharges of approximately 162 m^3 s^{-1} and 85 m^3 s^{-1}, respectively (ANA 2018). Based on the physical framework proposed by Dionne (1963) and Fairbridge (1980), the estuary can be subdivided into three longitudinal zones: a lower estuary dominated by marine processes, a middle estuary characterized by active mixing between fluvial and marine waters, and an upper estuary where tidal influence affects predominantly freshwater conditions.

The coastal plain surrounding the estuary is shaped by marine erosion and sedimentary processes, resulting in dynamic cliffs, cheniers, and extensive mangrove-dominated environments that promote sediment accumulation in low-energy zones (El-Robrini et al., 2006; Bandeira, 2013). The Turiaçu River basin is sparsely populated, with population density below 20 inhabitants km^{-2} and economic activities largely restricted to fishing and subsistence agriculture, indicating low anthropogenic pressure on the estuarine system (IBGE, 2022).

2.2 Water samples

Surface water samples were collected in 2018 along the longitudinal axis of the Turiaçu River estuary at four fixed stations (Figure 1), covering the main seasonal phases of the regional climate (February, April, July, and November). At each station, in situ measurements included temperature, pH, oxidation–reduction potential, dissolved oxygen, turbidity, and salinity. Water samples were also collected for laboratory determination of dissolved inorganic nutrients (NH_4^+, NO_2^-, NO_3^-, dissolved inorganic phosphorus, and silicate) and chlorophyll *a*.

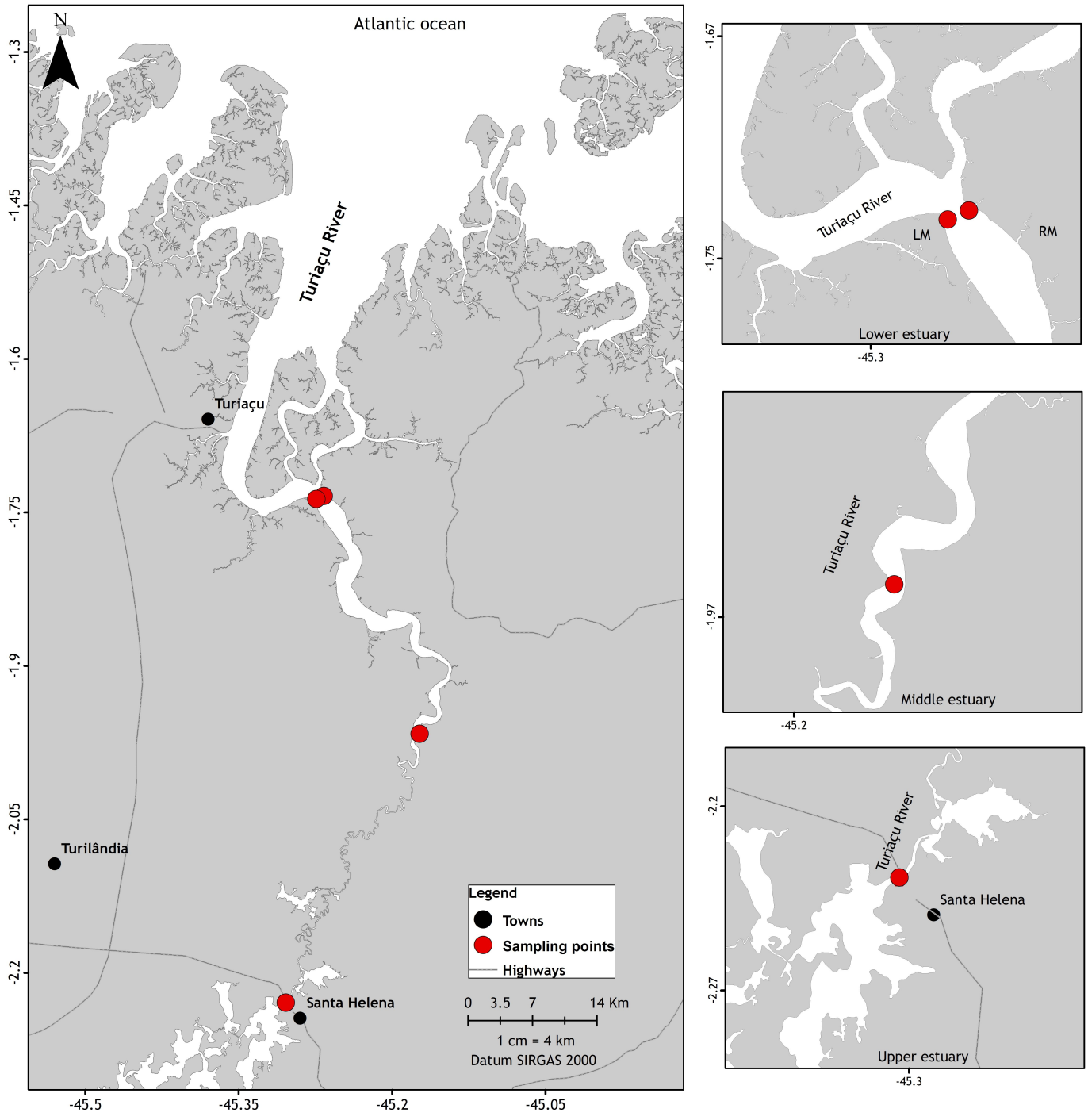


Figure 1. Study area in the Turiaçu River estuary during 2017 and 2018. The red square indicates the study region. The red dots indicate the water sample locations (N = 4).

All sampling campaigns were conducted during spring and quadrature tides, at flood and ebb, to standardize tidal conditions across the seasons and to record the maximum salinity gradient and biogeochemical transitions along the estuarine axis.

Sampling was restricted to four fixed longitudinal stations due to the extreme tidal currents (1–3 m s^{-1}), lack of safe navigation infrastructure, and the predominantly pristine nature of the system, which precludes road or bridge access. These stations were strategically positioned to capture the upper (1 station), middle (1 station), and lower estuarine zones (2 stations), representing the full salinity

gradient and the main biogeochemical transitions. Current velocity data were collected using an Acoustic Doppler Current Profiler (ADCP – Workhorse Rio Grande 1200 kHz) deployed on anchored vessels, with recordings at 0.5-second intervals (2 Hz).

2.3 Water quality analysis

Physical, chemical, and biological analyses were conducted at the LAPMAR laboratory facilities in Belém, Pará, Brazil. Salinity was measured using a Sea-Bird CTD (SBE-37SM), while temperature, pH, dissolved oxygen, oxidation–reduction potential, and turbidity were recorded in situ using a multiparameter probe (HORIBA U-52G). Surface water samples were collected with 10-L Van Dorn bottles, transferred to acid-cleaned containers, filtered through precombusted GF/F glass fibre filters (47 mm), and stored frozen (−20°C) until laboratory analysis.

Chlorophyll *a* was determined spectrophotometrically following Arar (1997). Dissolved inorganic nutrients (NH_4^+, NO_2^-, NO_3^-, PO_4^{3-}, and SiO_2) were analysed in triplicate according to Grasshoff et al. (1999) using a Quimis® Q898DRM spectrophotometer. Dissolved inorganic nitrogen (DIN) was calculated as the sum of NO_3^-, NO_2^-, and NH_4^+. Method detection limits were 0.05 μmol L^{-1} for NH_4^+, 0.06 μmol L^{-1} for NO_3^-, 0.04 μmol L^{-1} for NO_2^- and PO_4^{3-}, and 0.7 μmol L^{-1} for SiO_2.

2.4 DINX index

The relative availability of nitrogen and phosphorus was further assessed using the DINX index, which quantifies deviations from Redfield stoichiometry based on dissolved inorganic forms (Bates and Hansell, 2004; Hansell et al., 2004). DINX was calculated as:

$$\mathrm{DINX} = [NO_3^-] - 16\,[PO_4^{3-}]$$

Negative DINX values indicate nitrogen limitation relative to phosphorus, whereas positive values indicate an excess of nitrogen with respect to Redfieldian requirements for organic matter production.

2.5 Precipitation, fluvial discharge, and wind

Rainfall, river discharge, and wind direction data were obtained from meteorological and fluviometric stations within the Turiaçu River basin (Figure 2). Long-term datasets (1988–2018) were used to characterize regional climatological patterns and to support the interpretation of seasonal variability observed during the study period.

2.6 Biogeochemical model (LOICZ)

The LOICZ (Land–Ocean Interactions in the Coastal Zone) biogeochemical model was applied to estimate nutrient fluxes and ecosystem metabolism at the land–ocean interface based on steady-state mass-balance principles (Gordon et al., 1996; Swaney et al., 2011). The model assumes that water and salt behave conservatively, allowing water exchange between the estuary and the adjacent coastal ocean to be quantified using a salt budget, while dissolved inorganic nutrients behave non-conservatively due to internal biogeochemical processing (Giordani et al., 2008; Noriega and Araujo, 2011; Béjaoui et al., 2022).

The mass-balance calculations were performed sequentially. First, a water budget was constructed from freshwater inputs (river discharge, precipitation, and groundwater) and outputs (evaporation), yielding the residual flow (VR), which represents the net advective transport from the system to the sea. Second, a salt budget was

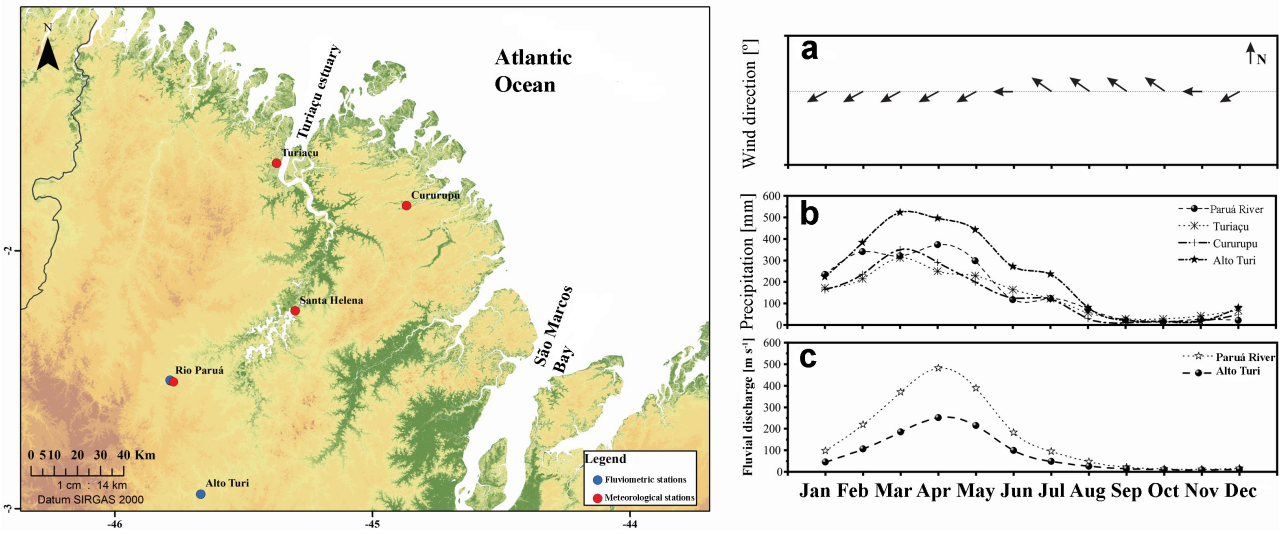


Figure 2. Climatological and fluviometric parameters in the Turiaçu River basin (1988–2018). a) Wind direction (°); b) rainfall (mm); c) fluvial discharge ($m^3\ s^{-1}$).

used to estimate the exchange flow (VX), a mixing term that accounts for tidal exchange between the estuary and the coastal ocean, calculated from the salinity gradient between the system and the sea. Third, budgets of dissolved inorganic phosphorus (DIP) and dissolved inorganic nitrogen (DIN) were calculated from water fluxes and concentration data. Deviations from conservative mixing (ΔDIP and ΔDIN) were interpreted as net internal sources or sinks of nutrients, reflecting the balance between biological and biogeochemical processes within the system.

Net ecosystem metabolism (NEM) was derived from ΔDIP using the Redfield C : P ratio (106 : 1), assuming that deviations in DIP primarily reflect net organic matter production (autotrophy, $\Delta DIP < 0$) or consumption (heterotrophy, $\Delta DIP > 0$). The net nitrogen balance (nitrogen fixation minus denitrification) was estimated as the difference between the observed ΔDIN and the DIN flux expected from stoichiometric coupling with ΔDIP, using the Redfield N : P ratio (16 : 1).

All calculations were performed using the LOICZ Simple Biogeochemical Budgets Calculator for a one–box, one–layer model (available at https://www2.arnes.si/~gljsentvid10/loicz_calculator.html), which follows the guidelines of Gordon et al. (1996). The complete set of equations used in the model is provided in the Supplementary Material (Text S1). This approach provides first-order estimates of estuarine metabolic status and nutrient processing under natural forcing conditions.

2.7 Statistical analysis

Descriptive statistics (mean, median, standard deviation, minimum, and maximum) were calculated for all variables. Because most datasets did not meet normality assumptions, non-parametric tests were applied, including the Mann–Whitney test, Kruskal–Wallis test, and Dunn's post hoc comparisons.

To further explore the relationships among physical, chemical, and biological variables, a Spearman correlation analysis was performed (rho; $p < 0.05$).

Statistical analyses were performed using PAST® software (Hammer et al., 2001), adopting a significance level of $p < 0.05$.

3. Results and discussion

3.1 Climatological context

Rainfall, river discharge, and wind patterns observed during the study period did not differ significantly from the long-term climatological record (1988–2018) (Mann–Whitney test, $p > 0.05$), indicating that the sampling year was representative of average regional conditions. Annual rainfall during the study period (~ 2,300 mm) was comparable to the historical mean (~ 2,150 mm), and river discharge values fell within the expected long-term range. Seasonal wind patterns were also consistent with historical observations, with dominance of southeast winds during the dry season and northwest winds during the rainy season. These results confirm that the hydrochemical variability observed in the estuary reflects natural seasonal forcing rather than anomalous climatic conditions. Climatological and hydrological data are presented in Figure 2.

3.2 Temperature and salinity

Water temperature and salinity variability along the Turiaçu River estuary is presented in Figure 3. Water temperature exhibited patterns typical of tropical estuaries, with higher mean values during the dry season (29.6 ± 0.6°C in November) and lower values during the wet season (26.7 ± 1.8°C in April) (Figure 3a). These values are comparable to those reported for other tropical hypertidal estuaries, such as São Marcos Bay (Lefèvre et al., 2017). Statistical analyses indicated significant seasonal differences in temperature ($p < 0.05$), reflecting the marked contrast between dry and rainy climatic periods. A mean thermal difference of approximately 3°C between these periods is consistent with observations from estuaries in northern and northeastern Brazil (Noriega and Araujo, 2014).

Salinity displayed a pronounced seasonal gradient, ranging from near freshwater conditions to fully marine waters (0–36 psu) over the annual cycle (Figure 3b). Higher

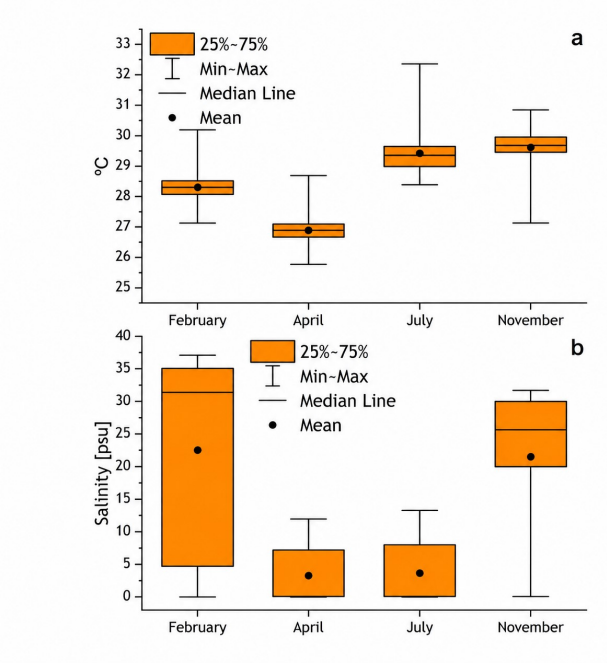


Figure 3. Boxplots of water temperature [°] (upper panel) and salinity (bottom panel) in the estuarine region of the Turiaçu River throughout the annual cycle. In the box, 25%–75% indicate the 25th and 75th percentiles, respectively. Min-Max indicates the minimum and maximum values, the Median line indicates the estimated median, and Mean indicates the average value of the series.

salinities were observed during the dry and transitional periods (November and February; mean ~ 30 psu), whereas values decreased sharply during the wet season (April and July; mean ~ 4 psu). This strong variability reflects the combined influence of intense freshwater discharge during peak rainfall and the hypertidal regime, which enhances mixing processes within the estuary. Significant differences in salinity among months ($p < 0.05$) highlight the strong seasonality of this parameter. The wider salinity range observed in February indicates transitional conditions, when both river discharge and tidal forcing exert substantial control on estuarine hydrography.

The spatial distribution of temperature and salinity across the four sampling stations is shown in Supplementary Material Figure S2a,b. Significant differences among stations were observed for both parameters (Kruskal–Wallis, $p < 0.001$; Table S3), with increasing salinity and temperature from the upper to the lower estuary, reflecting the transition from fluvial to marine conditions.

3.3 pH, dissolved oxygen (DO), ORP, turbidity and chlorophyll *a*

The pH values in the Turiaçu River estuary ranged from slightly acidic to alkaline conditions (5.0–9.0) over the annual cycle, with mean values close to neutrality (7.4 ± 0.5) (Figure 4a). Despite statistically significant seasonal differences ($p < 0.05$), pH variability remained relatively constrained, with most observations between 7.0 and 8.0. The predominance of neutral to slightly alkaline conditions indicates a strong marine influence associated with the hypertidal regime and reflects the natural chemical signature of a low-impact estuarine system. Observed pH values were higher than those reported for other estuaries in northern and northeastern Brazil (Noriega and Araujo, 2014) and were largely within the limits established by Brazilian environmental legislation for brackish waters (CONAMA, 2005).

Dissolved oxygen (DO) concentrations exhibited pronounced seasonal variability and generally low levels throughout the study period (Figure 4b). Mean DO values in all months were below the regulatory threshold of 5.0 mg L^{-1}, with fewer than 14% of samples exceeding this limit. Concentrations ranged from hypoxic to well-oxygenated conditions (0.3–12.7 mg L^{-1}), with the lowest values occurring during the dry and transitional periods (July and November) and higher values during the rainy season (February and April). Similar DO oscillations have been reported for the Turiaçu River and nearby estuarine systems, indicating that low oxygen levels are a recurrent feature of this region (Santos et al., 2019; Castellon et al., 2021).

The observed DO patterns are closely linked to water-column turbidity and redox conditions. Turbidity remained consistently high throughout the year, exceeding 100 NTU in all sampling periods and reaching an annual mean of approximately 322 NTU (Figure 4d). These values reflect intense sediment resuspension driven by strong tidal currents and river discharge, which limit light penetration and constrain photosynthetic oxygen production.

Spatial patterns of pH, DO, ORP, turbidity, and chlorophyll *a* across the four stations are provided in Supplementary Material Figure S2c–g. Turbidity was significantly higher at the Lower Left station ($p < 0.001$; Table S3), indicating localized sediment dynamics in this region. Dissolved oxygen was significantly lower in the upper estuary compared to other stations ($p < 0.01$), consistent with higher organic matter loading from riverine sources.

pH values also showed significant spatial variability ($p < 0.001$; Table S3), with higher values in the lower estuary compared to the upper estuary (Dunn's test, $p < 0.001$), reflecting the greater marine influence and the more alkaline conditions typical of coastal waters in the lower reaches of the system.

Oxidation–reduction potential (ORP) values were predominantly positive (> 200 mV), indicating a generally oxidizing environment and the absence of strongly reducing conditions (e.g., sulfide accumulation). Although ORP is not a direct proxy for dissolved oxygen concentration, positive ORP values are consistent with the predominance of oxidized species (such as O_2, NO_3^-, and metal oxides) in the water column. This apparent decoupling between ORP and low DO concentrations suggests that physical mixing and sediment dynamics—rather than biological oxygen consumption alone—play a dominant role in regulating both the redox state and oxygen availability in this hypertidal estuary (Figure 4c).

ORP shows significantly higher values in the lower estuary compared to the upper estuary ($p < 0.001$), consistent with the greater marine influence and more oxidizing conditions in the lower reaches of the system (Figure S2 and Supplementary Material, Table S3). Although light attenuation and primary production were not directly measured, the persistent high turbidity and consistently low chlorophyll *a* concentrations suggest that light limitation is the most plausible mechanism constraining photosynthetic oxygen production in this system (inferred from the observed inverse relationship between turbidity and DO).

Chlorophyll *a* concentrations were relatively low, with a mean annual value of 7.8 ± 10 mg m^{-3} (Figure 4e), consistent with mesotrophic conditions (Carmouze, 1994; Bricker et al., 2003). Significant seasonal differences were observed ($p < 0.05$), with higher values during February. Overall, low chlorophyll *a* concentrations appear to be primarily controlled by light limitation associated with persistent turbidity rather than by nutrient availability, a pattern also reported for other hypertidal systems such as São Marcos Bay (Lefèvre et al., 2017).

Chlorophyll *a* shows spatial variability, with higher values in the lower estuary (especially LL), suggesting that despite persistent turbidity, local conditions may favor

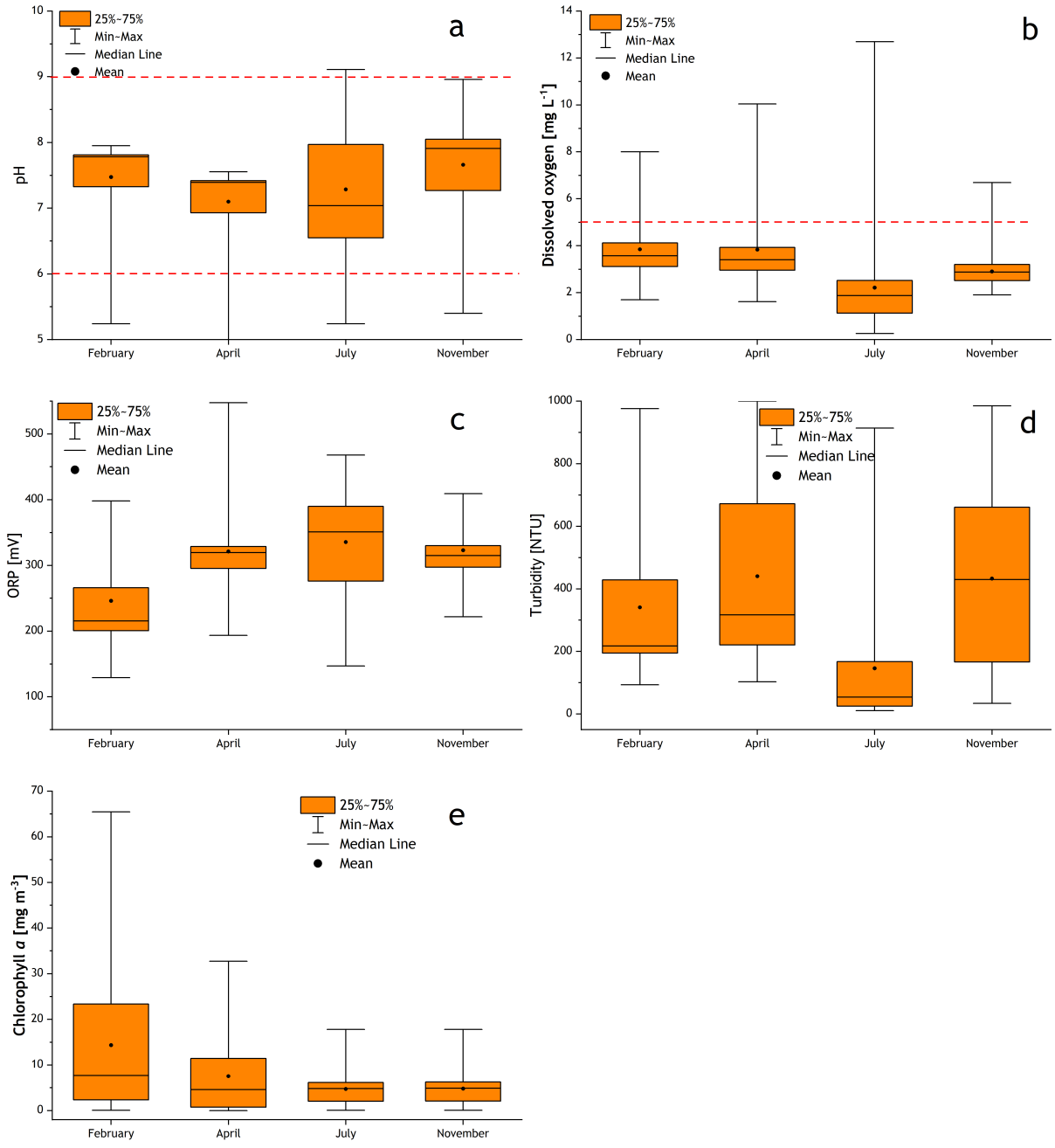


Figure 4. Boxplots of pH (a), DO (b), ORP (c), turbidity (d), and chlorophyll *a* (e) in the Turiaçu estuary. In the box, 25%–75% indicate percentile 25 and 75 respectively, Min–Max indicate minimum–maximum value, Median line indicates the estimated median; and Mean indicates the average value of the series.

phytoplankton growth in specific zones.

3.4 Nutrients (NH_4^+, NO_3^-, NO_2^-, PO_4^{3-} and SiO_2)

The concentrations of dissolved inorganic nitrogen, phosphorus, and silicate are shown in Figure 5. Ammonium (NH_4^+) concentrations were consistently low throughout the annual cycle, with maximum values below 10 μmol L^{-1}, well below the regulatory threshold for brackish waters (CONAMA, 2005) (Figure 5a). The CONAMA thresholds are established to protect aquatic biota from eutrophica-

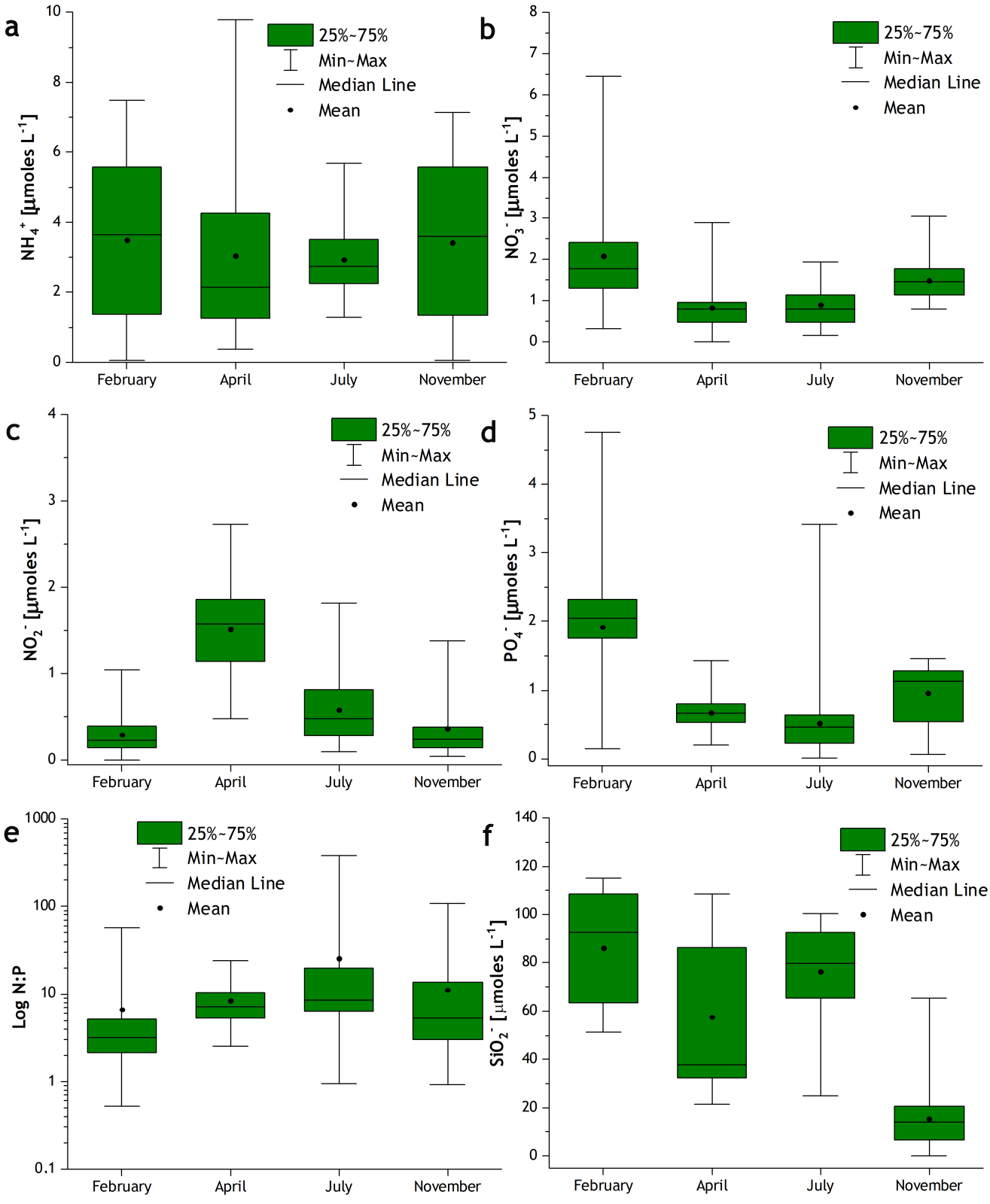


Figure 5. Box plots of the dissolved inorganic nutrient elements NH_4^+ (a), NO_3^- (b), NO_2^- (c), PO_4^{3-} (d), N : P ratio, in log values (e), and SiO_2^- (f) in the estuarine region of the Turiaçu River.

tion and toxicity effects; values consistently below these limits indicate the absence of nutrient enrichment and underscore the pristine, low-impact status of the Turiaçu estuary. No significant seasonal differences were observed (Kruskal-Wallis test, $p > 0.05$), and mean annual concentrations remained close to 3 μmol L^{-1}, indicating limited ammonification or rapid biological uptake.

Nitrate (NO_3^-) concentrations ranged from 0.1 to 6.5 μmol L^{-1} and also remained below regulatory limits for estuarine waters (Figure 5b). Although significant seasonal variability was detected (Kruskal–Wallis test, $p < 0.05$; followed by Dunn's post hoc test for pairwise comparisons), concentrations remained consistently low, with monthly means of 2.1 ± 1.46 μmol L^{-1} (February), 0.8 ± 0.45 μmol L^{-1} (April), 0.9 ± 0.48 μmol L^{-1} (July), and 1.5 ± 0.46 μmol L^{-1} (November), varying within a relatively narrow range (0.1–6.5 μmol L^{-1}) over the annual cycle. Higher values during February and November coincided with increased phytoplankton biomass (Figure 4e), suggesting enhanced biological uptake during periods of higher productivity.

Nitrite (NO_2^-) concentrations exhibited marked seasonal variability, ranging from 0.1 to 2.73 μmol L^{-1} (Figure 5c), with peak values observed in April, coinciding with maximum river discharge and turbidity. During this period, NO_2^- concentrations approached or exceeded the guideline value for brackish waters (CONAMA, 2005). Elevated turbidity and reduced dissolved oxygen likely inhibited complete nitrification, favouring the accumulation of NO_2^- in the water column. The predominance of the sequence $NH_4^+ > NO_3^- > NO_2^-$ contrasts with the typical estuarine pattern, where nitrate is usually the dominant dissolved inorganic nitrogen species in well-oxygenated waters (Bianchi, 2007) and suggests altered nitrification dynamics driven by intense sediment resuspension and light limitation in this hypertidal system.

Phosphate (PO_4^{3-}) concentrations varied from 0.01 to 4.8 μmol L^{-1}, with higher values recorded during the rainy period, particularly in February (Figure 5d). Mean annual concentrations (1.0 ± 0.5 μmol L^{-1}) remained below estimated guideline values for dissolved inorganic phosphorus, although episodic increases were observed during periods of high river discharge. Enhanced runoff and sediment resuspension during the wet season likely promoted the release of phosphorus from soils and bottom sediments, especially given the dominance of highly weathered latosols in the Turiaçu basin.

Seasonal variations in nitrogen and phosphorus resulted in pronounced deviations from the Redfield N : P ratio. Ratios $< 16:1$, and frequently $< 10:1$, were observed during periods of high rainfall and discharge (February and April), indicating nitrogen limitation, whereas ratios $> 16:1$ occurred during the drier period (July) (Figure 5e). Consistently negative DINX values across all seasons further indicate a deficit of dissolved inorganic nitrogen relative to phosphorus, suggesting that the Turiaçu estuary acts as a net source of phosphate to the adjacent coastal zone.

The consistently negative DINX values raise an important question: is nitrogen limitation primarily controlled by nutrient scarcity (biogeochemical control) or by physical constraints on nutrient uptake (hydrodynamic control)? We propose that both mechanisms operate in tandem in the Turiaçu estuary. The biogeochemical control is evidenced by the net denitrification fluxes estimated from the LOICZ budgets (Section 3.6), indicating that the system actively removes fixed nitrogen, particularly during periods of high river discharge. This process maintains a stoichiometric nitrogen deficit relative to phosphorus, as reflected by the DINX values. However, the hydrodynamic control is equally important: the relatively short water residence time (especially during the wet season; Table S2) limits the time available for biological assimilation, while persistent turbidity (> 100 NTU) attenuates light penetration, constraining phytoplankton growth irrespective of nutrient concentrations. Consequently, the low chlorophyll *a* levels observed (Section 3.3) are likely a combined result of limited nitrogen availability and physical constraints on primary production. This interpretation is consistent with findings from other hypertidal and high-turbidity systems, where physical forcing often overrides biological control of nutrient dynamics (Lefèvre et al., 2017; Costa, 2020).

Silicate (SiO_2) concentrations showed strong hydrological control, ranging from 0.03 to 115.1 μmol L^{-1}, with higher values during the rainy season and sharp declines during the dry period (Figure 5f). This pattern reflects the dominant role of leaching and river discharge in silicate supply. Observed concentrations and variability were comparable to those reported for the Amazon River and other tropical systems (Araujo et al., 2017; Aquino et al., 2022). The resulting stoichiometric ratios ($DIN : SiO_2 : PO^{3-} \approx 13 : 178 : 1$) strongly deviated from Redfield proportions and indicate nitrogen as the primary limiting nutrient, while phosphorus and silicate are supplied in relative excess, consistent with patterns reported for Amazon-influenced estuarine systems (Araujo et al., 2017).

3.5 Salinity gradient

The salinity gradient in the Turiaçu River estuary was analysed in relation to turbidity and nutrient distributions across all sampling periods and tidal conditions (Figure 6). High turbidity values were consistently observed along the salinity gradient during both spring and neap tides (Figure 6a,b), reflecting intense vertical and longitudinal mixing driven by the hypertidal regime.

Previous studies have shown that the lower (30–36 psu) and middle (5–30 psu) reaches of the Turiaçu estuary are predominantly well mixed to weakly stratified, with tidal energy exceeding river discharge, particularly during spring tides. Similarly, tidal currents reaching velocities of

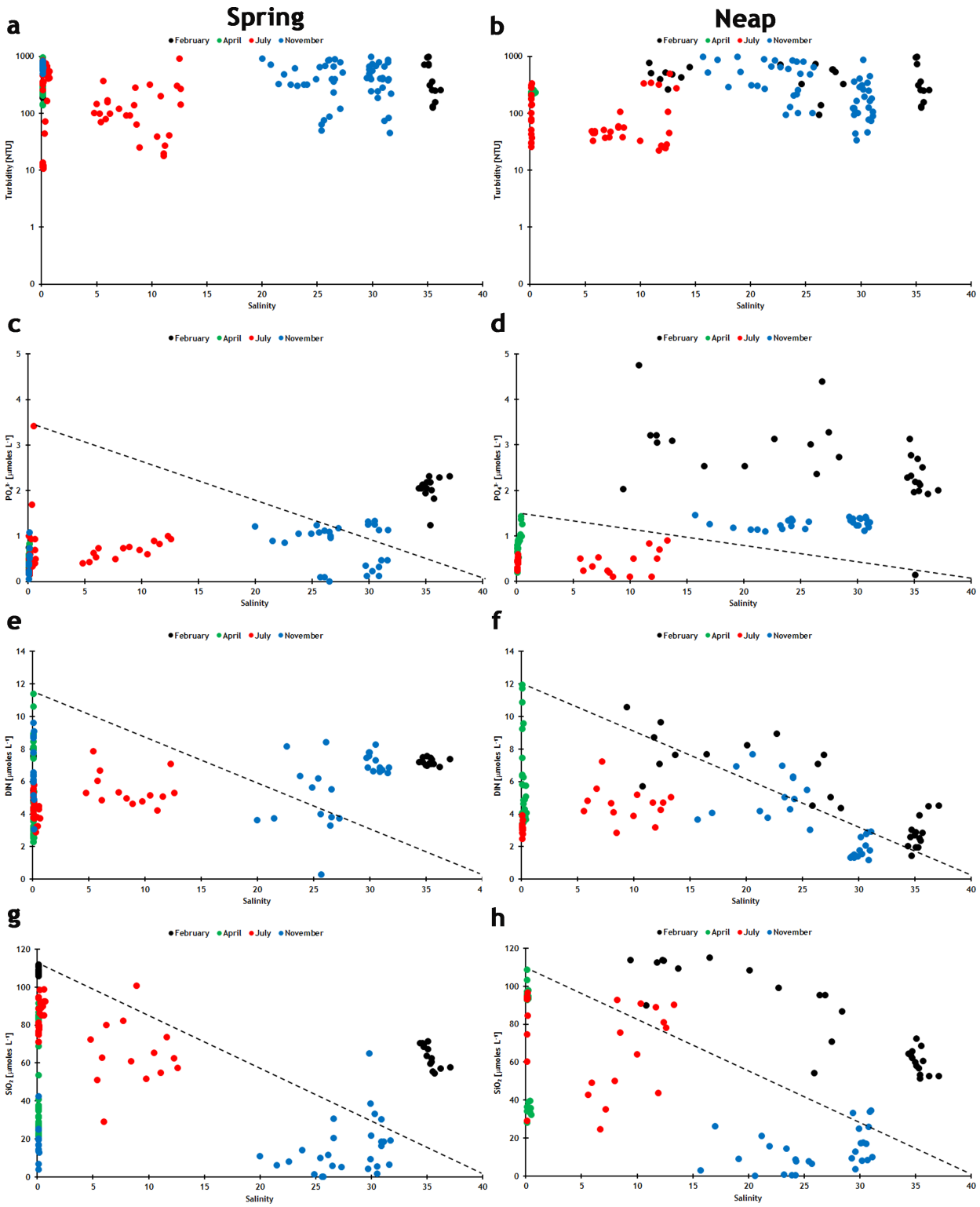


Figure 6. Distribution of turbidity (in Log values), PO_4^{3-}, DIN, and SiO_2 across the salinity gradient of the Turiaçu River estuary during spring and neap tides. The dashed line indicates the dilution pattern across the salinity gradient of a chemical element.

up to ~ 2 m s^{-1} promote strong resuspension of bottom sediments and suspended particulate matter, generating episodes of hyperturbidity, especially in the middle and lower estuary (Costa, 2020).

The persistent hyperturbidity observed in the Turiaçu estuary – exceeding 100 NTU throughout the year – distinguishes this system from most mesotidal tropical estuaries, where turbidity peaks are typically seasonal and river-driven. The combination of strong tidal currents (~ 1–3 m s^{-1}) and the seasonal variation in water residence time (shorter during the wet season; Table S2) promotes continuous sediment resuspension and non-conservative nutrient additions that are rarely observed in less energetic systems. Descriptive statistics of current velocities measured at the four sampling stations during each seasonal campaign are provided in Supplementary Material Table S1.

Although sampling was standardized at spring and quadrature tides, at flood and ebb, the inherent short-term variability of hypertidal systems (e.g., tidal pumping, sediment resuspension during ebb/flood cycles) may introduce additional intra-tidal variability not captured by our seasonal approach.

During the wet season, high river discharge (~ 180 m^3 s^{-1}; Costa, 2020) further enhances material transport toward the estuary, reducing retention time by approximately 61% (from 59 days in the dry season to 23 days in the wet season) (Table S1 and Table S2; supplementary material).

Supplementary Material Table S3 summarizes the results of non-parametric statistical comparisons (Kruskal–Wallis and Dunn's post hoc tests) among the four sampling stations for all variables, revealing significant spatial heterogeneity for most parameters ($p < 0.05$).

In summary, the salinity gradient and associated nutrient distributions in the Turiaçu estuary reveal a clear cascade of physical-biogeochemical coupling. The hypertidal regime drives intense sediment resuspension, which maintains persistent turbidity and promotes non-conservative nutrient additions in the middle and lower estuary. The seasonal variation in water residence time – shorter during the wet season (23 days) and longer during the dry season (59 days; Table S2) – modulates the extent of biological processing. During the wet season, the shorter residence time limits nutrient assimilation and organic matter degradation, favouring net nutrient export to the coast. In contrast, the longer residence time during the dry season allows greater biological processing, contributing to the observed metabolic shift towards autotrophy. This physical control is so dominant that it overrides the typical seasonal patterns of nutrient limitation observed in less energetic systems, reinforcing the interpretation that hydrodynamics – rather than biological uptake alone – are the primary drivers of nutrient dynamics in this system.

Along the estuarine gradient, phosphate (PO_4^{3-}) concentrations increased predominantly in the middle and lower estuary, particularly during neap tides (Figure 6c,d). This pattern suggests that sediment resuspension and intense mixing favour the release of phosphorus from particulate matter and organic-rich sediments, contributing to its addition along the salinity gradient.

Similarly, dissolved inorganic nitrogen (DIN) concentrations increased toward the middle and lower estuary (Figure 6e,f), indicating the dominant role of physical processes – tidal energy, mixing, and freshwater inflow – in controlling nutrient redistribution in this region.

Silicate (SiO_2) exhibited spatial and temporal patterns comparable to those of DIN and PO_4^{3-} (Figure 6g,h), although at substantially higher concentrations. These values are consistent with those reported for other Amazon-influenced estuaries, such as the Pará River estuary (Aquino et al., 2022), reinforcing the strong coupling between hydrological forcing, sediment dynamics, and silicate supply in hypertidal tropical systems.

The observations reported here highlight distinctive nutrient dynamics in a hypertidal estuary, where intense tidal energy in the middle and lower reaches exerts a primary control on the distribution of dissolved nutrients within the water column. These physical forcings strongly influence ecosystem metabolism by regulating the balance between organic matter production and respiration, which in turn governs the cycling of key nutrients such as nitrogen and phosphorus. To quantify these metabolic processes and their associated nutrient fluxes, we applied a simplified biogeochemical approach based on mass balance principles, incorporating river discharge, precipitation, evaporation, estuarine area and volume, salinity, and dissolved inorganic nutrients (PO_4^{3-} and DIN).

3.6 Estuarine metabolism

Estimates of estuarine metabolism were based on the stoichiometric framework of biogeochemical modelling using the canonical C : N : P ratio of 106 : 16 : 1, as recommended for seasonal assessments (Figure 7). The results indicate that the Turiaçu River estuary generally acts as a source of dissolved inorganic phosphorus (DIP; PO_4^{3-}) and dissolved inorganic nitrogen (DIN) to the adjacent coastal zone throughout the annual cycle (Figure 7a,b). Phosphate was exported during most of the year, except in November, when a negative flux (-0.01 mmol DIP m^{-2} d^{-1}) indicated temporary retention within the estuary. This reversal is associated with reduced river discharge, lower rainfall, and intensified tidal mixing during the dry season.

Exported DIP fluxes were substantially higher during February and April, with ΔDIP values ranging from 2.8 to 22.4×10^6 mol d^{-1}, whereas much lower or negative values were observed in July (0.4×10^6 mol d^{-1}) and November (-2.3×10^6 mol d^{-1}) (Figure 7a). According to the LOICZ methodology (Gordon et al., 1996), the C : P stoichiometric relationship ($\Delta DIC = \Delta DIP \times [C : P]$) indicates

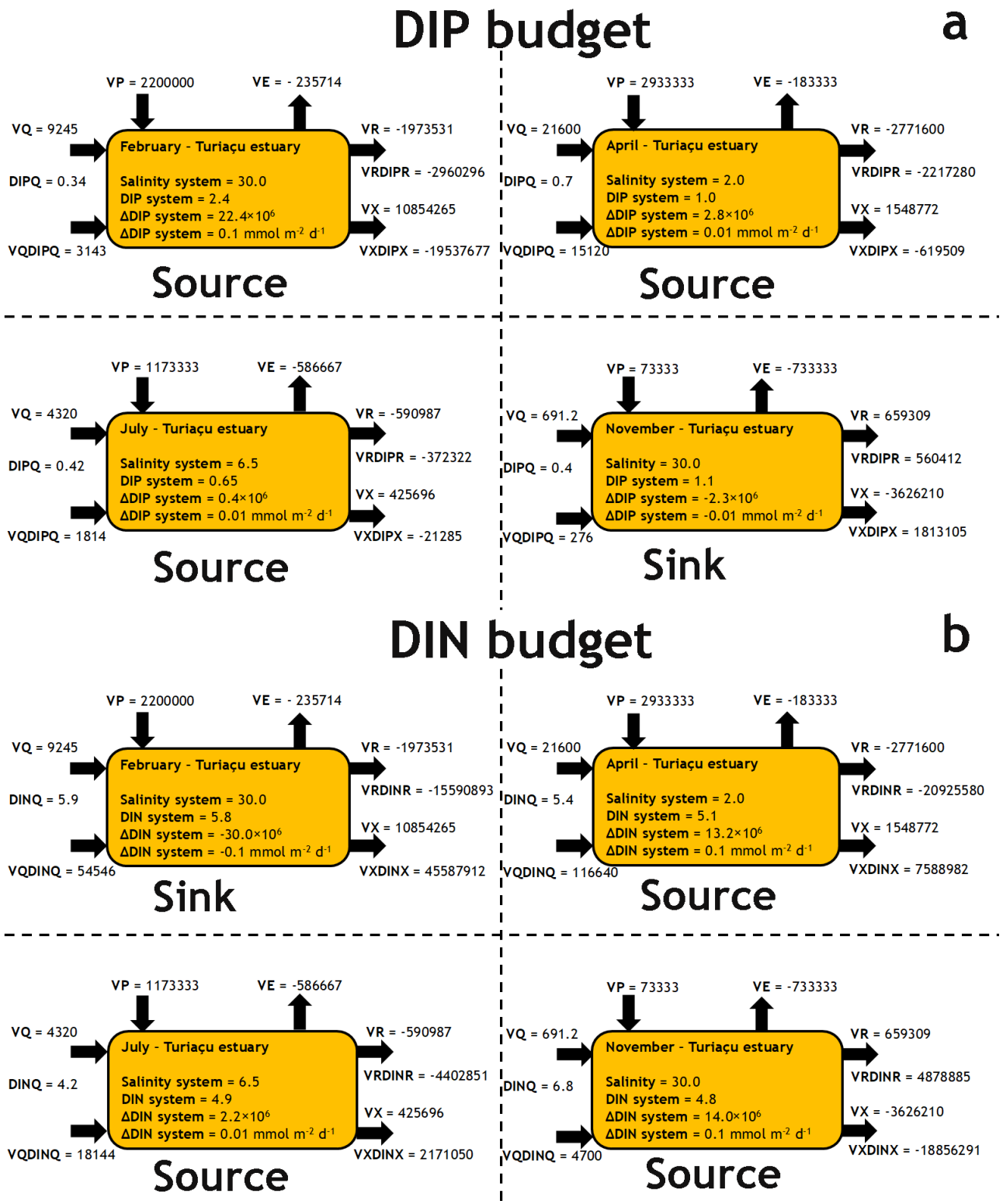


Figure 7. Seasonal mass balance of dissolved inorganic phosphorus (DIP; a) and dissolved inorganic nitrogen (DIN; b) in the Turiaçu River estuary. ΔDIP and ΔDIN represent the net fluxes across the land–ocean interface (10^6 mol d^{-1}). Runoff, precipitation, and evaporation are expressed in 10^3 m^3 d^{-1}. VQ, DIPQ, DINQ, VR, VX, VRDIYR, and VXDIYX are expressed in mol d^{-1} (DIY = DIP or DIN).

that the system alternated between heterotrophic and autotrophic states over the seasonal cycle.

During February and April, the estuary exhibited net heterotrophy, with NEM values of −10.6 and −1.1 mmol C $^{-2}$ d^{-1}, respectively, indicating that community respiration exceeded primary production and that the system acted as a net source of carbon to the atmosphere. Similar metabolic behaviour has been reported for other tropical estuaries in northern and northeastern Brazil, where mean CO_2 fluxes of 55 ± 45 mmol m^{-2} d^{-1}(range: 0.9–175.2 mmol m^{-2} d^{-1}) were observed, with higher emissions during the rainy season (Noriega and Araujo, 2014). In contrast, during July and November, the system shifted towards autotrophy, with positive NEM values of 0.01 and 1.1 mmol C m^{-2} d^{-1}, respectively, indicating net carbon uptake (P > R). In November, the mixing flow (V_x) changed sign, reflecting a reversal in estuarine–ocean exchange driven by enhanced tidal influence (Figure 7a).

Seasonal variations in DIN fluxes further revealed that the estuary predominantly acted as a DIN source to the coastal ocean, except in February, when the system functioned as a DIN sink (Figure 7b). During this month, higher DIN concentrations in river inflow (DINQ = 5.9 μmol L^{-1}) contributed to a negative ΔDIN. In April, July, and November, positive ΔDIN values indicated net export of DIN.

Using the LOICZ stoichiometric approach, the balance between nitrogen fixation and denitrification was estimated as the difference between observed and expected DIN fluxes [N fixation − denitrification = ΔDIN − ΔDIP × (N : P)]. The inferred nitrogen balance suggests that denitrification dominated during February (−1.7 mmol N m^{-2} d^{-1}) and April (−0.06 mmol N m^{-2} d^{-1}), whereas no dominant nitrogen transformation was detected in July due to low DIN fluxes. In November, the LOICZ budget indicates that nitrogen fixation prevailed, with a positive rate of 0.26 mmol N m^{-2} d^{-1}. These rates are consistent with values reported for other estuarine systems using similar modelling approaches.

Seasonal changes in salinity played a key role in modulating these biogeochemical processes. Salinity ranged from approximately 2 psu in April to 30 psu in February and November, indicating substantial variability in salt balance throughout the year (Figure 7). This variability reflects the combined effects of river discharge during periods of intense rainfall and the hypertidal regime, which alters mixing flows, residence time, and nutrient redistribution within the estuarine system.

We recognize that our nutrient measurements were restricted to surface waters, which may not capture potential vertical gradients in biogeochemical processes such as benthic regeneration or sediment–water fluxes. However, given the strong tidal mixing and shallow nature of the Turiaçu estuary, surface concentrations are likely representative of the bulk water column, supporting the use of the LOICZ mass-balance approach for first-order metabolic estimates. Future studies employing depth-resolved or continuous vertical profiling would help refine these estimates

3.7 Interrelationships among variables

To further explore the relationships among physical, chemical, and biological variables, a Spearman correlation analysis was performed (Supplementary Material Table S4). The analysis confirmed the strong hydrological control of the system, with salinity negatively correlated with silicate (rho = −0.31, $p < 0.05$) and nitrite (rho = −0.69, $p < 0.001$), indicating that these variables are enriched in freshwater-influenced waters. In contrast, phosphate (rho = 0.65, $p < 0.001$) and nitrate (rho = 0.60, $p < 0.001$) showed positive correlations with salinity, suggesting enrichment in the more saline lower estuary through sediment resuspension and desorption. Turbidity was positively correlated with nitrate (rho = 0.37, $p < 0.05$) and phosphate (rho = 0.28, $p < 0.05$), supporting the role of sediment resuspension in nutrient release. Importantly, no significant correlations were found between chlorophyll *a* and any of the dissolved inorganic nutrients (rho < 0.35, $p > 0.05$), reinforcing the interpretation that phytoplankton biomass is primarily controlled by physical factors – turbidity and light limitation – rather than by nutrient availability in this hypertidal system. As expected, NH_4^+ was strongly correlated with DIN (rho = 0.90, $p < 0.001$), consistent with its dominance among nitrogen species.

3.8 Implications for other systems

The findings from the Turiaçu estuary have implications beyond this single system. First, the quantitative nutrient flux estimates (ΔDIP and ΔDIN) contribute to the Global Nutrient Export from Watersheds (Global NEWS) model database, which currently lacks data from hypertidal tropical systems. Second, the observed metabolic alternation between heterotrophy and autotrophy provides a baseline for assessing future changes in other hypertidal systems under climate change and increasing anthropogenic pressure. Third, the methodological framework – combining seasonal hydrochemical observations with LOICZ mass-balance modelling – is transferable to other data-limited, high-energy coastal systems, particularly in tropical regions where logistical constraints limit extensive sampling. Regionally, this study establishes the first comprehensive hydrochemical baseline for the Maranhão coast, which can support future environmental licensing and conservation planning in an area experiencing rapid agricultural expansion.

4. Conclusion

This study analysed the hydrochemistry of the Turiaçu River estuary, northeastern Brazil, under a hypertidal regime, providing a comprehensive assessment of water

quality, nutrient dynamics, and estuarine metabolism in a system with low anthropogenic influence.

The results revealed pronounced seasonal variability in salinity, driven by the combined effects of intense tidal energy and river discharge during periods of higher rainfall. Persistent high turbidity in the mixing zone throughout the year strongly influenced dissolved oxygen, chlorophyll *a*, and nutrient concentrations, highlighting the dominant role of physical forcing in structuring estuarine biogeochemistry.

Nutrient distributions exhibited nonconservative behaviour along the salinity gradient, particularly in the middle and lower estuary. Dissolved inorganic phosphorus (DIP) and dissolved inorganic nitrogen (DIN) generally acted as sources to the adjacent coastal ocean, except in November (DIP sink) and February (DIN sink). Stoichiometric indicators (N : P ratios and DINX) consistently indicated nitrogen limitation for phytoplankton growth.

Silicate concentrations showed spatial and temporal patterns similar to those of other nutrients but at substantially higher magnitudes, resulting in elevated $SiO_2 : PO_4^{3-}$ ratios (39 : 1 to 457 : 1). Consequently, the overall DIN : $SiO_2 : PO_4^{3-}$ ratio (13 : 178 : 1) deviated markedly from the Redfield ratio, reflecting the strong influence of hydrological and sedimentary processes in this hypertidal estuary.

Biogeochemical modelling indicated that the estuary alternated between metabolic states over the seasonal cycle. During periods of high river discharge (February and April), the system was heterotrophic ($P < R$) and acted as a source of carbon to the atmosphere, whereas during July and November it shifted to autotrophy ($P > R$), functioning as a carbon sink. The inferred nitrogen balance indicates that denitrification dominated during the high-discharge months, while nitrogen fixation prevailed during the dry season.

Overall, the hydrochemical and metabolic patterns observed in the Turiaçu River estuary reflect biogeochemical processes typical of tropical hypertidal systems with minimal human impact, primarily controlled by the strength of tidal forcing and seasonal variability in river discharge.

Acknowledgements

We are grateful to ENAUTA (through clause PD&I of the ANP) for financing the project "North Coast – Development of methods for the understanding of the coastal processes, and the definition of the vulnerability of the mangroves of the basins of Pará and Maranhão, and the mouth of the Amazon".

The authors are grateful to the Unit of Laboratory Analysis (LAPMAR) of the Federal University of Pará for the analysis and data availability. C.N. thanks the Synthesis Center for Environmental and Climate Change – SIMACLIM (FINEP Grant 01.22.0584.00). M.A. acknowledges the support received from the Brazilian Research Network on Global Climate Change – Rede CLIMA (FINEP-CNPq 437167/2016-0).

Supplementary material

Supplementary material associated with this article can be found here.

Ethical approval

All authors have read, understood, and have complied, as applicable, with the statement on "Ethical responsibilities of Authors". Animal Ethics approval was not required for this research.

Conflict of interest

None declared.

References

Almeida, J., Bezerra, J.F., dos Santos, J., Moraes, M., Lisboa, G., 2022. *Avaliação das mudanças no uso da terra da Bacia Hidrográfica do Rio Turiaçu na região amazônica maranhense*. Rev. Bras. Geogr. Fís. 15 (1), 1965–1977.

Aguiar, V.M.C., Neto, J.A.B., Rangel, C.M., 2011. *Eutrophication and hypoxia in four streams discharging in Guanabara Bay, RJ, Brazil, a case study*. Mar. Pollut. Bull. 62(8), 1915–1919. https://doi.org/10.1016/j.marpolbul.2011.04.035

ANA – Agência Nacional das Águas, 2018. *HidroWeb*. Available at: http://hidroweb.ana.gov.br/ (accessed 12 January 2024).

Aquino, R., Noriega, C., Mascarenhas, A., Costa, M., Monteiro, S., Santana, L., Silva, I., Prestes, Y., Araujo, M., Rollnic, M., 2022. *Possible Amazonian contribution to Sargassum enhancement on the Amazon Continental Shelf*. Sci. Total Environ. 853, 158432. https://doi.org/10.1016/j.scitotenv.2022.158432

Arar, E.J., 1997. *Method 446.0: In vitro determination of chlorophylls a, b, $c_1 + c_2$ and pheopigments in marine and freshwater algae by visible spectrophotometry*. U.S. Environ. Protect. Agency, Washington, DC, 26 pp.

Araujo, M., Noriega, C., Hounsou-Gbo, G., Veleda, D., Araujo, J., Bruto, L., Feitosa, F., Flores-Montes, M., Lefèvre, N., Melo, P., Otsuka, A., Travassos, K., Schwamborn, R., Neumann-Leitão, S., 2017. *Assessment of the Amazon river–ocean continuum during boreal autumn: from physics to plankton communities and carbon flux*. Front. Microbiol. 8, 1358. https://doi.org/10.3389/fmicb.2017.01358

Araujo, M., Noriega, C., Lefèvre, N., 2014. *Nutrients and carbon fluxes in the estuaries of major rivers flowing into the tropical Atlantic*. Front. Mar. Sci. 1, 10. https://doi.org/10.3389/fmars.2014.00010

Archer, A.W., 2013. *World's highest tides: hypertidal coastal systems in North America, South America and Europe*.

Sediment. Geol. 284–285, 1–25. https://doi.org/10.1016/j.sedgeo.2012.12.007

Bandeira, I.C.N., 2013. *Geodiversidade do estado do Maranhão*. CPRM – Programa Geologia do Brasil, 294 pp.

Bates, N.R., Hansell, D.A., 2004. *Temporal variability of excess nitrate and nitrogen fixation in the subtropical North Atlantic*. Mar. Chem. 84, 225–241. https://doi.org/10.1016/j.marchem.2003.08.003

Béjaoui, B., Basti, L., Melaku Canu, D., Feki-Sahnoun, W., Salem, H., Dahmani, S., Sahbani, S., Benabdallah, S., Blake, R., Norouzi, H., Solidoro, C., 2022. *Hydrology, biogeochemistry and metabolism in a semi-arid Mediterranean coastal wetland ecosystem*. Sci. Rep. 12, 9367. https://doi.org/10.1038/s41598-022-12936-5

Bianchi, T.S., 2007. *Biogeochemistry of estuaries*. Oxford Univ. Press, New York, 706 pp.

Bricker, S.B., Ferreira, J.G., Simas, T., 2003. *An integrated methodology for assessment of estuarine trophic status*. Ecol. Modell. 169, 39–60. https://doi.org/10.1016/S0304-3800(03)00199-6

Carmouze, J.P., 1994. *O metabolismo dos ecossistemas aquáticos: fundamentos teóricos, métodos de estudo e análises químicas*. FAPESP, São Paulo, 253 pp.

Castellon, S., Cattanio, J.H., Berredo, J., Rollnic, M., Neu, V., Ribeiro, M., 2021. *Spatial and temporal variability of carbon dioxide and methane fluxes in an Amazonian estuary*. Int. J. Hydro. 5 (6), 327–336. https://doi.org/10.15406/ijh.2021.05.00294

CONAMA – Conselho Nacional do Meio Ambiente, 2005. *Resolução CONAMA nº. 357, de 17 de março de 2005*. Available at: https://www.icmbio.gov.br/cepsul (accessed 3 January 2024).

Costa, M., 2020. *Influência da hipermaré sobre os processos hidro-sedimentares: estudo de caso no estuário do Rio Turiaçu – MA*. Ph. D. Thes., Federal Univ. Pará, 109 pp.

Dionne, J.C., 1963. *Towards a more adequate definition of the St. Lawrence estuary*. Z. Geomorphol. 7 (1), 36–44.

El-Robrini, M., Silva, M.M., El-Robrini, M.H., Feitosa, A.C., Tarouco, J.E.F., dos Santos, J.H.S., Viana, J.R., 2006. *Maranhão*. [In:] Muehe, D. (Ed.), *Erosão e progradação no litoral brasileiro*. MMA, Brasília, 87–130.

Fairbridge, R.W., 1980. *The estuary: its definition and geodynamic cycle*. [In:] Olausson, E., Cato, I. (Eds.), *Chemistry and biogeochemistry of estuaries*. John Wiley & Sons, New York, 1–35.

FEMAR – Fundação de Estudos do Mar, 2017. *Catálogo de estações maregráficas: estação de Turiaçu*. Available at: http://www.fundacaofemar.org.br (accessed 16 January 2024).

Giordani, G., Austoni, M., Zaldívar, J.M., Swaney, D.P., Viaroli, P., 2008. *Modelling ecosystem functions and properties at different time and spatial scales in shallow coastal lagoons: An application of the LOICZ biogeochemical model*. Estuar. Coast. Shelf Sci. 77 (2), 264–277. https://doi.org/10.1016/j.ecss.2007.09.017

Gordon, D.C., Boudreau, P.R., Mann, K.H., Ong, J.-E., Silvert, W.L., Smith, S.V., Wattayakorn, G., Wulff, F., Yanagi, T., 1996. *LOICZ biogeochemical modelling guidelines*. LOICZ Rep. Stud. 5, Texel, The Netherlands, 105 pp.

Grasshoff, K., Ehrhardt, M., Kremling, K., 1999. *Methods of seawater analysis*, 3rd edn. Wiley-VCH, Weinheim.

Hammer, Ø., Harper, D.A.T., Ryan, P.D., 2001. *PAST: Paleontological statistics software package for education and data analysis*. Palaeontol. Electron. 4 (1), 9 pp.

Han, C., Qiu, S., Li, X., Ke, Y., Vogt, R.D., Lu X, 2026. *Estuarine Mixing Drives Organic Nitrogen Transformation and Bioavailability Dynamics*. EGUsphere 2026-216. https://doi.org/10.5194/egusphere-2026-216

Hansell, D.A., Bates, N.R., Olson, D.B., 2004. *Excess nitrate and nitrogen fixation in the North Atlantic*. Mar. Chem. 84, 243–265. https://doi.org/10.1016/j.marchem.2003.08.004

IBGE – Instituto Brasileiro de Geografia e Estatística, 2022. *Population estimates*. Available at: https://www.ibge.gov.br (accessed 16 January 2024).

INMET – Instituto Nacional de Meteorologia, 2018. *Banco de Dados Meteorológicos*. Available at: http://www.inmet.gov.br (accessed 10 January 2024).

Kirby, R., 2010. *Distribution, transport and exchanges of fine sediment, with tidal power implications: Severn Estuary*, UK. Mar. Pollut. Bull. 61, 21–36. https://doi.org/10.1016/j.marpolbul.2009.12.011

Lefèvre, N., Dias, F.J., Torres Jr., A., Noriega, C., Araujo, M., Castro, A., Rocha, C., Jiang, S., Ibánhez, J.S., 2017. *A source of CO_2 to the atmosphere throughout the year in the Maranhense continental shelf (2°30′S, Brazil)*. Cont. Shelf Res. 141, 38–50. https://doi.org/10.1016/j.csr.2017.05.004

Li, S., Bush, R.T., 2015. *Revision of methane and carbon dioxide emissions from inland waters in India*. Global Change Biol. 21, 6–8.

Nogueira, N., 2003. *Estrutura da comunidade fitoplanctônica em cinco lagos marginais do rio Turiaçu (Maranhão, Brasil) e sua relação com o pulso de inundação*. M. Sc. Thes., Federal Univ. São Carlos, 122 pp.

Noriega, C., Araujo, M., 2011. *Nutrient budgets (C, N and P) and trophic dynamics of a Brazilian tropical estuary: Barra das Jangadas*. An. Acad. Bras. Ciênc. 83 (2), 441–456. https://doi.org/10.1590/S0001-37652011000200007

Noriega, C., Araujo, M., 2014. *Carbon dioxide emissions from estuaries of northern and northeastern Brazil*. Sci. Rep. 4, 6164. https://doi.org/10.1038/srep06164

Santos, M., Neulls, T., Vieira, L., Gonçalves, P., Figueiredo, I., 2019. *Análise do monitoramento da qualidade da água do Rio Turiaçu no Estado do Maranhão*. V Fórum Latino-Americano de Engenharia e Sustentabilidade.

https://doi.org/10.29327/15304

Smith, S.V., Swaney, D.P., Talaue-McManus, L., 2010. *Carbon–Nitrogen–Phosphorus Fluxes in the Coastal Zone: The LOICZ Approach to Global Assessment*. [In:] Liu, K.K., Atkinson, L., Quiñones, R., Talaue-McManus, L. (Eds.), *Carbon and Nutrient Fluxes in Continental Margins*. Springer, Berlin, Heidelberg. https://doi.org/10.1007/978-3-540-92735-8_14

Swaney, D.P., Smith, S.V., Wulff, F., 2011. *The LOICZ Biogeochemical Modeling Protocol and its Application to Estuarine Ecosystems*. [In:] Wolanski, E., McLusky, D. (Eds.), *Treatise on Estuarine and Coastal Science*. Acad. Press, 135–159. https://doi.org/10.1016/B978-0-12-374711-2.00907-4

Thrush, S.F., Townsend, M., Hewitt, J.E., Davies, K., Lohrer, A.M., Lundquist, C., Cartner, K., 2013. *The many uses and values of estuarine ecosystems*. [In:] Dymond, J.R. (Ed.), *Ecosystem services in New Zealand – conditions and trends*. Manaaki Whenua Press, Lincoln, New Zealand, 356–367.

Torres, A.M., El-Robrini, M., 2006. *Amapá*. [In:] Muehe, D. (Ed.), *Erosão e progradação no litoral brasileiro*. MMA, Brasília, 11–40.

Uncles, R.J., Stephens, J.A., Harris, C., 2013. *Estimating estuarine turbidity: an application to estuaries of the Isle of Man and northeast Irish Sea*. Ocean Coast. Manag. 79, 42–51. https://doi.org/10.1016/j.ocecoaman.2012.05.013

Uncles, R.J., Stephens, J.A., Smith, R.E., 2002. *The dependence of estuarine turbidity on tidal intrusion length, tidal range and residence time*. Cont. Shelf Res. 22, 1835–1856. https://doi.org/10.1016/S0278-4343(02)00041-9